

Extraction of Dynamic Inflow Models for Coaxial and Tandem Rotors from CFD Simulations

Po-Wei Chen

aweberchen@gatech.edu

Research Assistant

School of Aerospace Engineering,
Georgia Institute of Technology,
Atlanta, GA, USA

Natasha L. Schatzman

natasha.schatzman@nasa.gov

Aerospace Engineer

NASA Ames Research Center
Mountain View, CA, USA

Lakshmi N. Sankar

lsankar@ae.gatech.edu

Professor

School of Aerospace Engineering,
Georgia Institute of Technology,
Atlanta, GA, USA

JVR Prasad

jvr.prasad@ae.gatech.edu

Professor

School of Aerospace Engineering,
Georgia Institute of Technology,
Atlanta, GA, USA

R. Ganesh Rajagopalan

rajagopa@iastate.edu

Professor

Iowa State University
Ames, IA, USA

INTRODUCTION

The dynamic inflow coupling with rotor/body dynamics is crucial in the analysis of stability and control law design for helicopters. Over the past several decades, finite-state inflow models for single rotor configurations in hover, forward flight, and maneuver have developed(Ref.1, 2). By capturing the interference effects between rotors, the extension of pressure potential finite state inflow model has promising result for coaxial rotor configuration(Ref.3). Recently, the focus of the dynamic inflow modeling has shifted from coaxial to tandem rotor configurations (Ref.4, 5). The development of the dynamic inflow models for tandem rotor configuration still have some limitations due to the lack of knowledge of rotor-to-rotor and rotor-wake interference. Experimental methods, and computational fluid dynamics methods are commonly used to understand the rotor performance and rotor airload variations, and predict inflow velocity distributions at the rotor disk. The inflow distributions are subsequently used to improve the dynamic inflow models.

Tandem rotor configurations have been studied experimentally and computationally for several decades(Ref.6, 7). Sweet (Ref.6) observed that a tandem rotor with 76-percent-radius overlap required 14% more induced power at hovering condition, relative to an isolated rotor of equivalent disk area. Sweet also found that, above a shaft-to-shaft distance of 1.03 diameter, the performance of the tandem rotor was nearly the same as two isolated rotors.

The objective of the present study is to apply computational fluid dynamic simulations of tandem rotors for the extraction of dynamic inflow models. The extended methodology is first validated by comparing the computed induced power against test data. Subsequently inflow distributions and wake structures are analyzed.

CFD METHODOLOGIES

Numerical simulations are prone to inherent errors (arising from discretization error in space and time), artificial diffusion of the wake structures, and empirical constants that are used in turbulence models. Development of dynamic inflow models based on a single CFD model therefore would not result in a physically accurate inflow model. These errors may be reduced, and confidence in the inflow model may be improved, if two or more CFD methodologies that are different in their approach but complementary to each other. For this reason, two CFD methodologies (GT-Hybrid and RotCFD) are being used in this work.

GT-Hybrid employs a hybrid wake methodology, meaning that the flow field is only resolved within a small gridded domain surrounding a single rotor blade. Within this grid, the discretized Navier-Stokes solutions are found using a time-accurate flux-limited MUSCL scheme with 3rd order spatial and 1st order temporal accuracy. The turbulence model used here is the Spalart-Allmaras Detached Eddy Simulation (SA-DES) model. The specific parameters for the SA-DES model has been chosen for the balance of accuracy and computational time required (Ref.8). Outside of this small gridded domain, the wakes of other blades are efficiently modelled with a free wake model.

RotCFD is widely used in the rotorcraft industry (Ref.7). With a user-friendly graphic user interface (GUI) user can access Rot3DC structured solver or RotUNC unstructured solver. The flow solver in RotUNC is a finite volume based SIMPLE solution algorithm for pressure-velocity coupling. The solver uses a k- ϵ turbulence model. Two options are available to model the rotor: an actuator disk model, or a discrete blade model. The present work uses the discrete blade model. Both options rely on user-provided tables of two-dimensional airfoil coefficients for a range of angle-

of-attack and Mach number. Using the computed velocity field and blade element momentum theory, the local angle-of-attack and the Mach number at each blade element section is computed and the aerodynamic coefficients are retrieved from the airfoil tables. The section forces and moments are then converted to source terms that are added to the momentum equations at the grid cells that encompass the blade section.

COAXIAL ROTOR MODEL

The coaxial Harrington rotor 1 with diameter of 25 ft. is modeled in this study. The single and coaxial Harrington rotor 1 were tested at Langley full-scale wind tunnel in 1951 (Ref.9). The rotor separation distance is 2.33 and the solidity for the coaxial rotor is 0.054. The Harrington rotor 1 has 2 blades each rotor with untwist and linear taper from root to tip of 0.35. Figure 1 shows the airfoil shape for several radial sections are chosen to model the Harrington rotor 1.

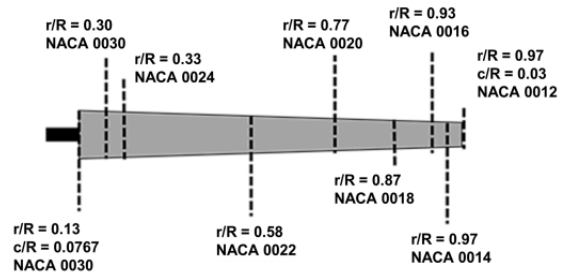


Figure 1. Blade geometry of Harrington rotor 1

TANDEM ROTOR MODEL

The tandem rotor with untwisted rectangular and NACA 0012 airfoil sections throughout the blade is modeled in this study because of the availability of test data (Ref.6). As shown in Figure 2, the front rotor (blue) is rotating in the counter-clockwise direction (when viewed from above the helicopter), and the rear rotor (red) is rotating in the clockwise direction. The blades are initially placed with a 90 degree difference as shown below. Both the rotors have an identical radius of 7.62 feet, and an identical solidity of 0.0968. L is the shaft-to-shaft length and the D is the diameter of the rotor. In the experiments (Ref.6), the tandem rotor configuration has no vertical offset. Two cases with overlapping and non-overlapping cases are studied. The corresponding length-to-diameter values for non-overlapping and the overlapping cases are 1.03 and 0.63, respectively. For the overlapping rotor case, the total disk area is reduced by 13.4%.

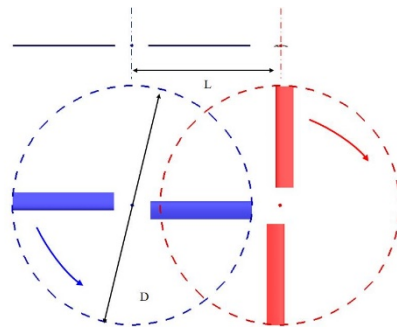


Figure 2. Tandem rotor configuration with 13.4% area overlap

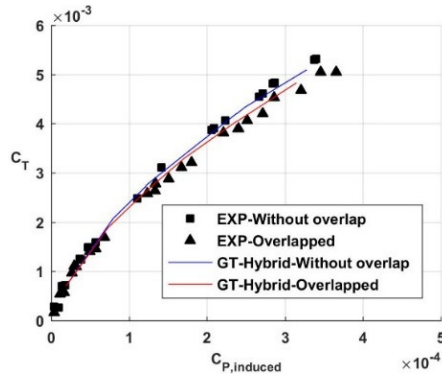


Figure 3. Comparison of computed and measured induced power versus thrust coefficient for tandem rotor in hover (experimental data from Sweet)

induced power, compared against the test data. Reasonable agreement is observed. In particular, the rise in the induced power due to rotor overlap is well captured by the simulations.

The inflow velocity distribution at the rotor disk is available from the simulations as a function of space and time. Figure 4 shows the inflow velocity contours for coaxial Harrington rotor 1 in hover for both upper and lower rotors. The inflow velocity for the lower rotor has interference from the wake of the upper rotor.

Figure 5 shows the representative inflow velocity contours for the tandem rotor in hover, for both the front and the rear rotor for non-overlapping case. While there are radial variations in the inflow, it is seen that the inflow velocity is nearly uniform with respect to the azimuth except in the region of interference - near zero degree azimuth for the front rotor and 180 degree azimuth for the rear rotor. As the overlap increases, the interference effects substantially

PRELIMINARY RESULTS

Both GT-Hybrid and RotCFD have computed the performance of the coaxial Harrington rotor 1 in hover and forward flight (Ref.10, 11). Although published results are, for the most part, related to rotor performance and pressure fields, inflow distributions are also available. This data is valuable for development and assessment of inflow models.

Calculations have been completed using GT-Hybrid model for tandem rotors in hover and forward flight. RotCFD calculations are in progress. For brevity, only the hover results from GT-Hybrid are shown in this abstract. The full paper will include results from RotCFD simulations and the forward flight results.

The test data could be split into profile power and induced power components. Because inflow model is of primary interest in the present study, our focus is on the induced power component, which serves as a surrogate for the inflow. Figure 3 shows the predicted data for the

increase. Figure 6 shows the time-averaged induced velocity for both the front and rear rotor disks. A significant increase in the downwash velocity magnitude is seen. The kinetic energy expended in this increased downwash manifests itself as an increase in the induced power, resulting in a 15% higher induced power.

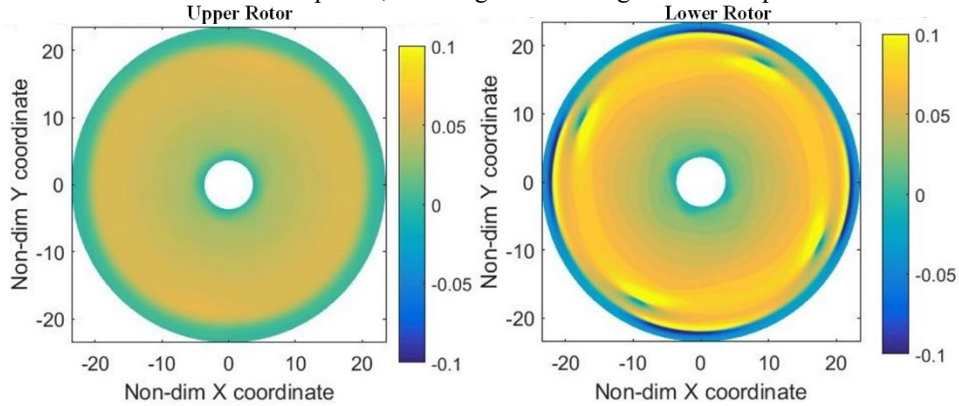


Figure 4. GT-Hybrid prediction of the inflow on the disk for coaxial Harrington Rotor 1

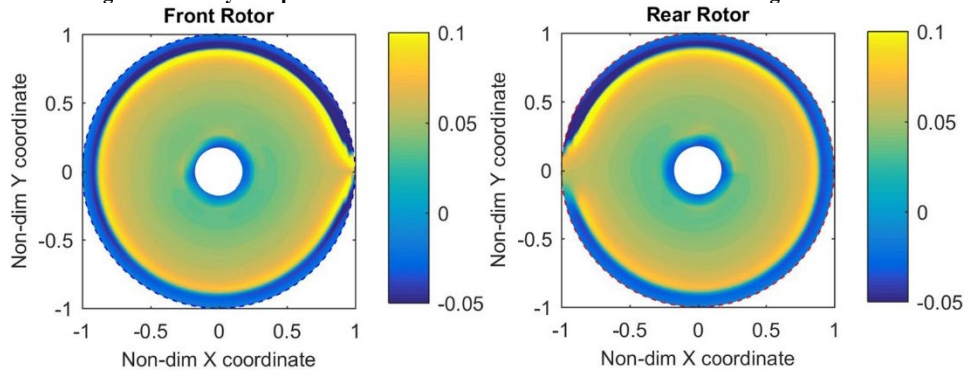


Figure 5. GT-Hybrid prediction of the inflow on the disk for non-overlapped tandem rotor

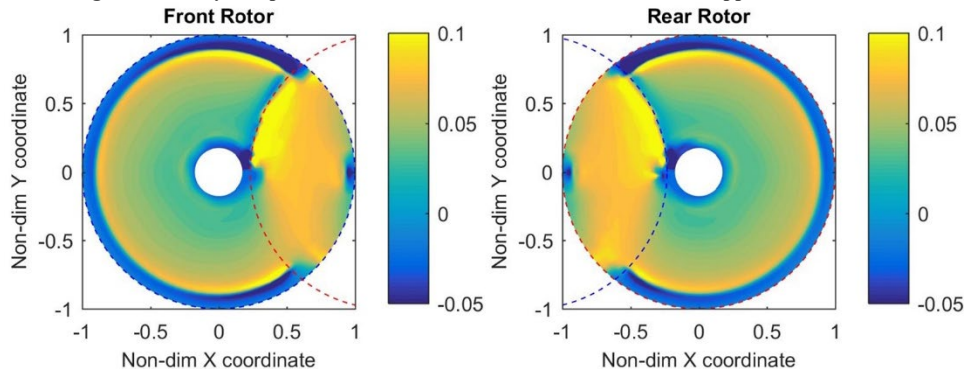


Figure 6. GT-Hybrid prediction of the inflow on the disk for overlapped tandem rotor

In Figure 7(a), the tip vortex structure for a reference blade is shown at a representative time. The solid lines in the vicinity of the rotor blade tip represent the strong tip vortex trajectory, while the lattice structure corresponds to the inner wake. It is seen that the tip vortices from the front and rear rotor both descend slowly compared to the inner wake. It is also seen that the inner wake has a linear variation in the descent rate from root to tip, so that the outer edge of the inner wake (close to the blade tip) descends faster than the inner edge close to the root. These features have been experimentally observed by Gray (Ref.12) and several other researchers (Ref.13). It is also seen that the tip vortices from the front and rear rotor interact with each other, and pushed upwards towards the rotor disk. They may also have a cancelling effect as far as the upwash outboard of the tip vortex goes, as seen in the previous figure. Figure 7 (b) shows the tip vortex for reference blades on the front and rear rotor, and its associated inner wake. As expected, it is seen that there is significant interaction between the tip vortices, which are quite strong. There are significant interactions also between the inner wake structure of the front rotor and the tip vortices from the rear rotor, and vice versa.

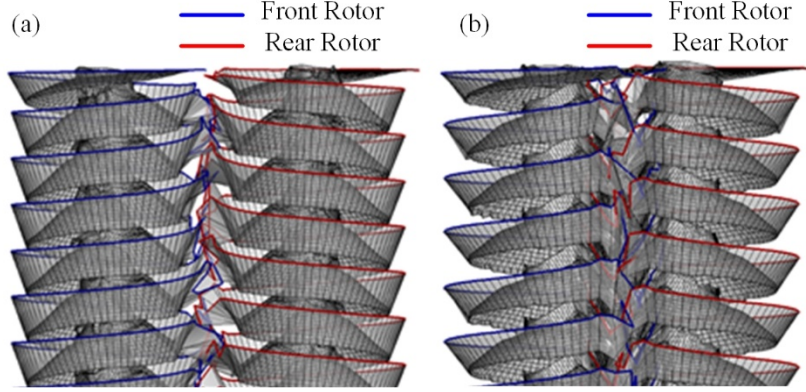


Figure 7. The wake structure for (a) non-overlapped and (b) overlapped tandem rotor case.

EXTRACTION OF DYNAMIC INFLOW MODELS

The CFD simulations shown in Figures 4-6 are functions of non-dimensional radial (\vec{r}) and azimuthal locations (ψ). They are not directly useful in flight simulations which rely on efficient dynamic inflow models for rapid, real-time simulations. The following methodology is used to reduce the data from CFD approach (Ref. 14).

The induced velocity $\bar{v}_z(\vec{r}, \psi)$ at the rotor disk, normalized by the tip speed, is related to the mean thrust, and the rolling and pitching moments generated by the rotor at the hub. We may view the induced velocity as series in terms of the non-dimensional radial location (\vec{r}) and the azimuthal location (ψ). The first few terms of this series are:

$$\bar{v}_z(\vec{r}, \psi) = \lambda_0 + \lambda_{1c}\vec{r}\cos(\psi) + \lambda_{1s}\vec{r}\sin(\psi)$$

Since the induced velocity is available from CFD simulations, we may compute λ_0 , λ_{1c} , and λ_{1s} as:

$$\lambda_0 = \frac{1}{\pi} \int_0^{2\pi} \int_0^1 \bar{v}_z(\vec{r}, \psi) \vec{r} d\vec{r} d\psi$$

$$\lambda_{1c} = \frac{4}{\pi} \int_0^{2\pi} \int_0^1 \bar{v}_z(\vec{r}, \psi) \vec{r}^2 \cos(\psi) d\vec{r} d\psi$$

$$\lambda_{1s} = \frac{4}{\pi} \int_0^{2\pi} \int_0^1 \bar{v}_z(\vec{r}, \psi) \vec{r}^2 \sin(\psi) d\vec{r} d\psi$$

For the tandem and coaxial rotors in hover considered here, the inflow would be predominantly uniform in the azimuthal direction. The components, λ_{1c} , and λ_{1s} thus serve as a measure of the interference effects.

CURRENT STATUS OF THE WORK

Only a small subset of our results for tandem and coaxial rotors in hover has been shown here for brevity. The full paper will include:

1. Comparison of RotCFD and GT-Hybrid results for inflow and wake structure in hover and in forward flight
2. Extraction of the dynamic inflow model coefficients for the Harrington rotor and the tandem rotor
3. Comparisons of inflow models with those developed from viscous vortex particle methods (Ref.14).

PRIOR PUBLICATION

Inflow for the tandem rotor in hover published at the 7th Asian-Australian Rotorcraft Forum (Ref.15). This work extends the previous study to tandem rotors in forward flight, and to coaxial rotors in hover and forward flight. The development of a dynamic inflow model will be included in present study. The comparison of dynamic inflow models from two different CFD approaches (GT Hybrid and RotCFD) will be present to reduce the influence of numerical discretization errors on inflow models.

ACKNOWLEDGMENTS

This project was funded by the U. S. Army under the Vertical Lift Research Center of Excellence (VLRCOE)

program managed by the National Rotorcraft Technology Center, Aviation and Missile Research, Development and Engineering Center under Cooperative Agreement W911W6-06-2-0004 between Georgia Institute of Technology and the U. S. Army Aviation Applied Technology Directorate. Dr. Mahendra Bhagwat is the technical monitor. The authors would like to acknowledge that this research and development was accomplished with the support and guidance of the NRTC. The views and conclusions contained in this document are those of the authors and should not be interpreted as representing the official policies, either expressed or implied, of the Aviation and Missile Research, Development and Engineering Center or the U.S. Government.

REFERENCES

- ¹He, C. J., "Development and application of a generalized dynamic wake theory for lifting rotors," Ph.D. Thesis, School of Aerospace Engineering, Georgia Institute of Technology, Atlanta, GA, 1989.
- ²Peters, D. A. and He, C. J., "Correlation of measured induced velocities with a finite-state wake model," *Journal of the American Helicopter Society*, Vol. 36, (3), pp. 59-70, 1991. doi: 10.4050/JAHS.36.59
- ³Nowak, M., Prasad, J. V. R., Xin, H., and Peters, D. A., "A potential flow model for coaxial rotors in forward flight," 39th European Rotorcraft Forum, Moscow, Russia, September 3-6, 2013
- ⁴Kong, Y. B., Prasad, J. V. R., and Peters, D. A., "Analysis of a Finite State Multi-Rotor Dynamic Inflow Model," 43rd European Rotorcraft Forum, Milan, Italy, September 12-15, 2017.
- ⁵Guner, F., Kong, Y. B., Prasad, J. V. R., Peters, D. A., and He, C. J., "Development of Finite State Inflow Models for Multi-Rotor Configurations using Analytical Approach," American Helicopter Society 74th Annual Forum, Phoenix, Arizona, May 14-17, 2018
- ⁶Sweet, G. E., "Hovering measurements for twin-rotor configurations with and without overlap," NACA TN D-534, 1960.
- ⁷Rajagopalan, R. G., Baskaran, V., Hollingsworth, A., Lestari, A., Garrick, D., Solis, E., and Hagerty, B., "RotCFD-A tool for aerodynamic interference of rotors: Validation and capabilities," Future Vertical Lift Aircraft Design Conference, San Francisco, CA, January 18-20, 2012
- ⁸Marpu, R. P., Sankar, L. N., Makinen, S. M., Egolf, T. A., Baeder, J. D., and Wasikowski, M., "Physics-based modeling of maneuver loads for rotor and hub design," *Journal of Aircraft*, Vol. 51, (2), pp. 377-389, 2014. doi: 10.2514/1.C031843
- ⁹Harrington, R. D., "Full-scale-tunnel Investigation of the Static-thrust Performance of a Coaxial Helicopter Rotor," NACA-TN-2318, 1951.
- ¹⁰Barbely, N. L., Komerath, N. M., and Novak, L. A., "A study of coaxial rotor performance and flow field characteristics," American Helicopter Society Aeromechanics Specialist's Conference, San Francisco, CA, January 20-22, 2016
- ¹¹Kim, J., Sankar, L., and Prasad, J., "Application of a Navier-Stokes free wake hybrid methodology to the Harrington coaxial rotor," American Helicopter Society Specialists Conference on Aeromechanics Design for Vertical Lift, San Francisco, CA, January 20-22, 2016
- ¹²Gray, R. B., "An aerodynamic analysis of a single bladed rotor in hovering and low-speed forward flight as determined from smoke studies of the vorticity distribution in the wake," Ph. D. Thesis, Aeronautical Engineering Department, Princeton University, Princeton, NJ, 1956.
- ¹³Landgrebe, A. J., "The wake geometry of a hovering helicopter rotor and its influence on rotor performance," *Journal of the American Helicopter Society*, Vol. 17, (4), pp. 3-15, 1972. doi: 10.4050/JAHS.17.3
- ¹⁴Guner, F., Prasad, J. V. R., Sankar, L., Peters, D. A., and He, C. J., "Correlation of Finite State Multi-Rotor Dynamic Inflow Models with a High Fidelity Viscous Vortex Particle Method," Proceedings of the 44th European Rotorcraft Forum, Delft, The Netherlands, September 19-20, 2018
- ¹⁵Chen, P. W., Sankar, L., and Prasad, J. V. R., "A Hybrid Navier Stokes - Free Wake Method for Modeling Tandem Rotors," Proceedings of the 7th Asian-Australian Rotorcraft Forum, Jeju Island, Korea, October 30 - November 1, 2018